

KINETICS AND MECHANISM OF THERMAL
DECOMPOSITION OF COBALT (II), NICKEL (II) AND COPPER
(II) CINNAMATE COMPLEXES IN DYNAMIC NITROGEN
ATMOSPHERE

by

H. Moselhy *

The High Institute for Engineering, Chemical Engineering Department, P.O. Box 3, El-Shorouk City, Cairo, Egypt

ABSTRACT

The thermal decomposition of cinnamate complexes of cobalt (II), nickel (II) and copper (II) was carried out using thermogravimetry (TG), derivative thermogravimetry (DTG) and differential scanning calorimetry (DSC). The kinetics and mechanism of the decomposition process were evaluated. The different stages of decomposition were identified from TG and DTG. The kinetic parameters were evaluated from TG curves using Coats-Redfren equation. For cobalt and nickel cinnamate the decomposition process follows the mechanism of three-dimensional diffusion D_3 while copper cinnamate decomposition mechanism follows the random nucleation mechanism F_1 with the formation of one nucleus on each particle (Mamplé equation). The heat of reaction for the decomposition process was determined using DSC.

* To whom all correspondences should be addressed.

INTRODUCTION

Recently, increasing interest has been devoted to the thermal decomposition of transition metal carboxylate complexes in solid state¹⁻⁵. Both isothermal and non-isothermal methods have been used to evaluate the kinetics and the mechanism of their thermal decomposition reaction⁶. The present article reports the synthesis and thermal behavior of Co (II), Ni (II) and Cu (II), cinnamate complexes together with their kinetic and mechanistic aspects of their thermal degradation in the solid phase using non-isothermal TG techniques.

EXPERIMENTAL

The cinnamate of cobalt (II), nickel (II) and copper (II) complexes were prepared using the corresponding metal carbonate. A hot solution of cinnamic acid was prepared and then the metal carbonate was added with vigorous stirring. Excess metal carbonate was filtered off. The filtrate was concentrated over a steambath until the complex crystallized and then separated and washed with hot water.

Metal contents were assayed using a Varian AA-1475 series atomic absorption spectrophotometer. C, H analyses were determined using a Carlo Erba elemental analyzer model 1106. Data were given in Table 1. IR spectra was obtained using KBr discs on a Pye-Unicam SP3-300 IR spectrophotometer (4000-200 cm^{-1}).

TG, DTG thermal studies were carried out on TA-3000 Mettler thermobalance with a heating rate Q of $10^\circ\text{C min}^{-1}$ and 10 mg sample weight. The TG cell was fed with N_2 gas with a flow rate of 50 ml NTP min^{-1} in temperature range 50-990°C. The DSC analyzer was a DSC-30mettler system. Thermograms were taken under experimental conditions as in TG except the

final temperature was 590°C and sample weight 6 mg. Non-isothermal TG data were processed.

Table (1). Analytical data of cinnamate complexes

Complexes	Color	C%		H%		M%	
		Found	Calculated	Found	Calculated	Found	Calculated
Co (C ₉ H ₇ O ₂) ₂ ·2H ₂ O	Pink	55.49	55.49	4.59	4.62	15.50	15.13
Ni (C ₉ H ₇ O ₂) ₂ ·2H ₂ O	Green	54.92	55.52	4.73	4.62	15.14	15.08
Cu (C ₉ H ₇ O ₂) ₂	Blue	59.94	60.42	3.63	3.95	17.42	17.75

RESULTS AND DISCUSSION

Elemental analyses of the complexes show that the complexes have the chemical formula of M (C₉H₇O₂)₂·XH₂O where X=2 for either cobalt (II) or nickel (II) while copper (II) complexes reveals anhydrous nature. In Fig. 1, IR spectra assigned bands their location were cited in Table 2.

Table (2). The assigned spectral vibration bands for the cinnamate complexes

Compounds	ν_{OH} (br.s)	ν_{COOH}	ν_{COO}	$\nu_{C=C}$	ν_{C-O}	ν_{M-O}
C ₉ H ₈ O ₂		1660s		1610(s)	1410(s)	
Co(C ₉ H ₇ O ₂) ₂ ·2H ₂ O	3600 - 2900		1550(s)	1610(s)	1410(s)	280 s
Ni (C ₉ H ₇ O ₂) ₂ ·2H ₂ O	3600 - 2800		1550(s)	1615(s)	1410(s)	280 m
Cu (C ₉ H ₇ O ₂) ₂			1550(s)	1625(s)	1410(s)	280 m

Table 2, shows the absence of carboxylic group vibrational band in the IR spectra of the complexes while the C = C vibrational band still existing besides the formation of M-O bonds. This will confirm that co-ordination of cinnamic acid with metal ions proceeded via COO⁻ ions. The electronic spectra of these

complexes have been studied ^{7, 8} and confirmed an octahedral environment with a polymeric nature ⁹.

TG and DTG analyses were conducted in N₂ atmosphere in order to prevent the oxidative decomposition of the fragments. Analytical and mass loss calculations are cited in Table 3 . The table shows that dehydration of water of crystallization has been occurred first then followed by the ligand decomposition in three distinct processes . Values of temperature of inception (T_i), temperature of completion of each process (T_f) and its maximum (T_m) are given in Table (3).

Table (3). TG and DTG phenomenological data for thermal decomposition of cinnamate complexes in N₂ atmosphere

stage	Decomposition mode	T _i	T _f	T _m	%wt loss
I- cinnamic acid (C₉H₈O₂)					
1	1 mol C ₆ H ₆ + 1 mol CO ₂	123	217	203	81.91
2	1 mol C ₂ H ₂	217	309	241	18.09
Total loss % = 100					
II- cobal cinnamate Co(C₉H₇O₂)₂ . 2H₂O					
1	2 mol H ₂ O	75	174	145	9.84
2	2 mol C ₆ H ₅ ⁻ + 2 mol CO	272	473	372	54.19
3	2 mol C ₂ H ₂ + 1/2 mol O ₂	473	728	548	18.16
4	addition of 1/2 mol O ₂	736	768	827	+4.95
5		827	894	882	+2.95
residue Co ₂ O ₃		Total loss % = 82.19			

III- nickel cinnamate $\text{Ni}(\text{C}_9\text{H}_7\text{O}_2)_2 \cdot 2\text{H}_2\text{O}$

1	$\cong 2 \text{ mol H}_2\text{O}$	50	188	77	6.10
2	2 mol C_6H_5 + 2 mol C_2H_2 + 2 mol CO	246	493	424	64.76
3	1/2 mol O_2	493	584	536	4.87
4	addition of 1/2 mol O_2	929	679	970	+3.83
	residue NiO				Total loss % = 75.73

IV-copper-cinnamate $\text{Cu}(\text{C}_9\text{H}_7\text{O}_2)_2$

1	1 mol C_6H_5	199	287	294	21.49
2	1 mol C_6H_5 + 2 mol C_2H_2 + 1 mol CO	294	487	309	46.50
	residue CuCO_3				Total loss % = 67.99

TG curve for cinnamic acid as in Fig.2 starts at 123°C and ended in two distinct stages with a total volatilization of the acid. The first stage comprises a total loss of 81.91% that is mainly due to removal of one mole C_6H_6 and one mole CO_2 . This stage is followed by removal of one mole C_2H_2 . DTG curve for the same sample shows that removal of the first two degradation products occurred in one broad and sharp peak followed by a smaller one which is corresponding to the removal of C_2H_2 polymerized form⁹.

TG and DTG decomposition pattern of cobalt (II) cinnamate complex as in Fig.3 differs from that of the cinnamic acid. Three stages of degradation were occurred. Spectroscopic and magnetic data⁵ predict that these complexes have planner arrangements with the carboxylate group of two different cinnamate ions bonded to a metal atom to give one layer that makes the C_6H_5 ring free out of the plane of the layer, thus, facilitating its decomposition. Evidently shown that prolonged heating of the cobalt (II) complex up to 730°C causes interaction of the residue with oxygen forming Co_2O_3 oxide.

Nickel (II) cinnamate TG and DTG decomposition (Fig.4) show the same mode of decomposition as in cobalt complex. Dehydration process occurred

early with temperature difference of about 25°C while the complex decomposition temperature was retarded due to the stability of nickel (II) complex with the formation of nickel oxide as a final product. Since copper (II) cinnamate complex has no water of crystallization, thus, the mode of decomposition seems to be different. Two TG decomposition stages were obtained as in Fig. 5 with the formation of copper metal as a final product. DSC thermograms of the degradation of the complexes were shown in Figs. 2-4. The corresponding values of temperature of each stage and their enthalpies were cited in Table 4.

Table (4). DSC temperature and ΔH for the thermal decomposition cinnamate Complexes

Compounds	Stage	TEMPERATURE °C	ΔH J G ⁻¹
1-malonic acid	I	135	171.2 (endo)
	II	277	397 (endo)
			Total = 3456.9 (endo)
2-cobalt cinnmate	I	146	285 (endo)
	II	268	25.1 (exo)
	III	328	243 (endo)
			Total = 2210.0 (endo)
3-nickel cinnamate	I	83.4	151.10 (endo)
	II	305	26.40 (endo)
	III	435	37.73 (endo)
	IV	521	42.30 (endo)
			Total = 908.20 (endo)
4-copper cinnamate	I	223	27.6 (endo)
	II	286	202.0 (endo)
			Total = 2386.7 (endo)

As shown in Table 4, values of ΔH_{total} for the complexes were less than the ΔH_{total} for the decomposition of the cinnamic acid. This can confirm the autocatalytic decomposition of the complexes. The retarded decomposition temperature of the nickel (II) complex (stage II) can be due to its thermodynamic stability. Also, the DSC data obtained for copper (II) cinnamate can illustrate different mechanism of decomposition. This can be declared through deduction of the reaction mechanism for non-isothermal methods, which has been discussed by Sestak and Berggren¹⁰. Kinetic parameters are evaluated from non-isothermal TG curves by application of the Arrhenius equation :

$$d\alpha/dT = A/Q \exp[-E/RT] f(\alpha)$$

A series of $f(\alpha)$ forms are proposed¹¹ and the mechanism is obtained from the one that gives the best representation of the experimental data. In this study the Coats-Redfren method was used for solving the exponential integral. E and A were calculated in each case from the slope and intercept in the following equation¹² respectively

$$\ln [g(\alpha)/T^2] = \ln [AR/QE (1 - 2 RT/E)] - E/RT$$

The entropy of activation (ΔS) was calculated from the equation

$$A = [K T_s / h] \exp [\Delta s / R]$$

Where T is the temperature (K), A is the pre-exponential factor, Q is the heating rate ($^{\circ}\text{C min}^{-1}$), E is the energy of activation, R is the gas constant, T_s is the DTG peak temperature, K is the Boltzman constant and h is Plank's constant.

The values of E and A obtained for the mechanistic equation along with the correlation co-efficient (r) for the kinetic plots are reported in Table 5. It can be seen that the highest values of the correlation coefficients obtained for the total decomposition process up to $\alpha = 0.7$ are the mechanism of three dimensional diffusion D_3 for either cobalt or nickel cinnamate. While for copper cinnamate decomposition, it follows the random nucleation mechanism (F_1) with the formation of one nucleus on each particle (Mamplé equation). It seems that

the absence of water of crystallization for the complex affects its mechanism during thermal decomposition.

The values of ΔS which are included in Table 5 show a negative values of entropy, this indicate that for these complexes decomposition of the activated complex has a more, ordered structure than the reactant and the reaction in these cases may be ascribed as slower than normal ¹³.

Table (5). Kinetic parameters for the decomposition of Co (II), Ni (II) and Cu (II) cinnamate complexes using mechanistic equation from TG in a flow of nitrogen atmosphere.

Mechanistic g(α) employed	from of g(α)	parameter	cinnamate complex of		
			Co II	Ni II	Cu II
D ₁	α^2	E KJ mol ⁻¹	47.56	85.63	98.10
		A S ⁻¹	6.59x10 ⁵	2.24x10 ³	5.24x10 ⁷
		r	0.983	0.991	0.981
D ₂	$\alpha+(1-\alpha) \ln(1-\alpha)$	E	54.21	93.94	108.91
		A	3.69x10 ⁵	6.91x10 ³	6.03x10 ⁸
		r	0.986	0.993	0.985
D ₃	$1-(1-\alpha)^{1/3}$	E	62.86	103.92	124.71
		A	3.29x10 ⁵	1.42x10 ⁴	1.28x10 ¹⁰
		r	0.989	0.994	0.990
D ₄	$(1-2/3\alpha)-(1-\alpha)^{2/3}$	E	57.03	99.76	113.90
		A	9.76x10 ⁵	3.26x10 ³	5.77x10 ⁸
		r	0.987	0.992	0.987
R ₁	$1-(1-\alpha)$	E	17.88	37.41	44.89
		A	1.85x10 ⁷	1.25x10 ⁶	7.42x10 ³
		r	0.969	0.993	0.978
R ₂	$1-(1-\alpha)^{1/2}$	E	23.36	44.06	54.04

		A	1.52×10^7	6.89×10^5	1.28×10^3
		r	0.978	0.991	0.986
R_3	$1-(1-\alpha)^{1/3}$	E	25.44	46.56	58.45
		A	1.61×10^7	6.46×10^5	2.05×10^3
		r	0.981	0.984	0.990
A_2	$[-\ln(1-\alpha)]^{1/2}$	E	9.15	20.78	29.93
		A	2.28×10^7	6.39×10^6	9.64×10^4
		r	0.981	0.984	0.990
A_3	$[-\ln(1-\alpha)]^{1/3}$	E	2.19	9.98	17.45
		A	1.70×10^7	1.80×10^7	1.25×10^6
		r	0.822	0.875	0.888
F_1	$-\ln(1-\alpha)$	E	30.01	52.38	68.17
		A	2.44×10^6	7.81×10^4	9.48×10^4
		r	0.98	0.998	0.993
		S JK ⁻¹ mol ⁻¹	-142.1	-166.8	-155.0

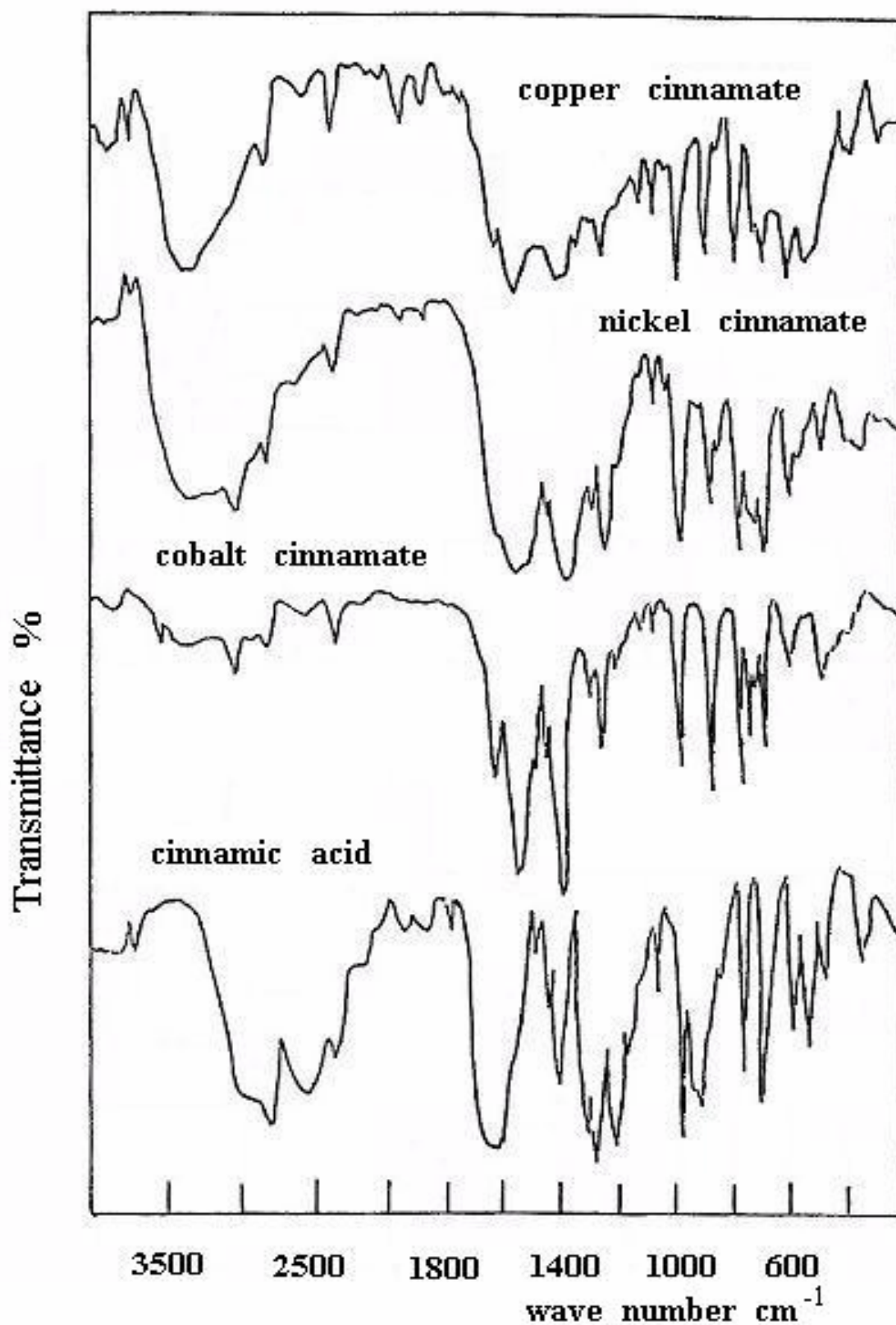


Fig. 1. IR spectra of cinnamate complexes.

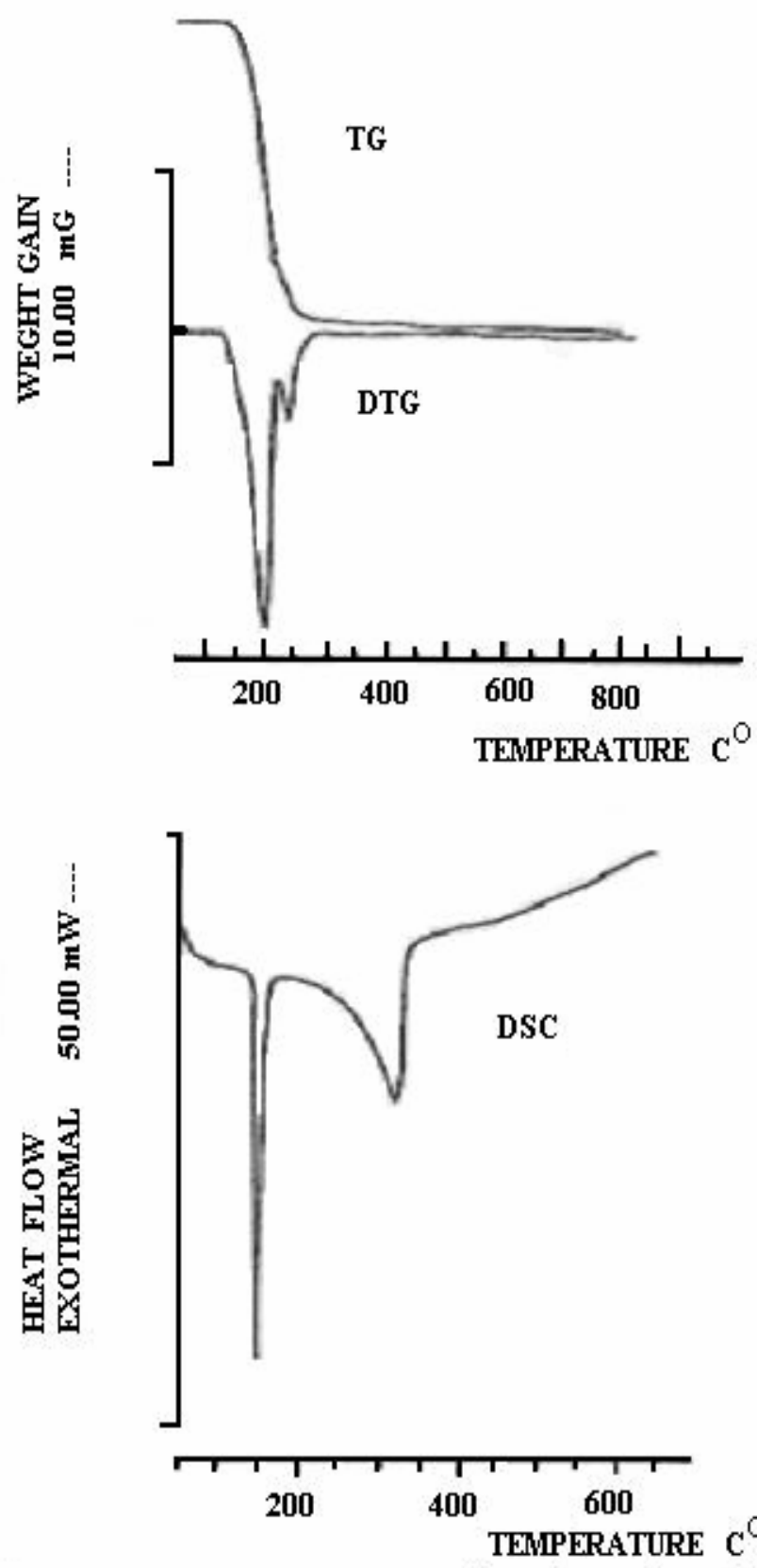


Fig.2. TG, DTG and DSC for cinnamic acid .

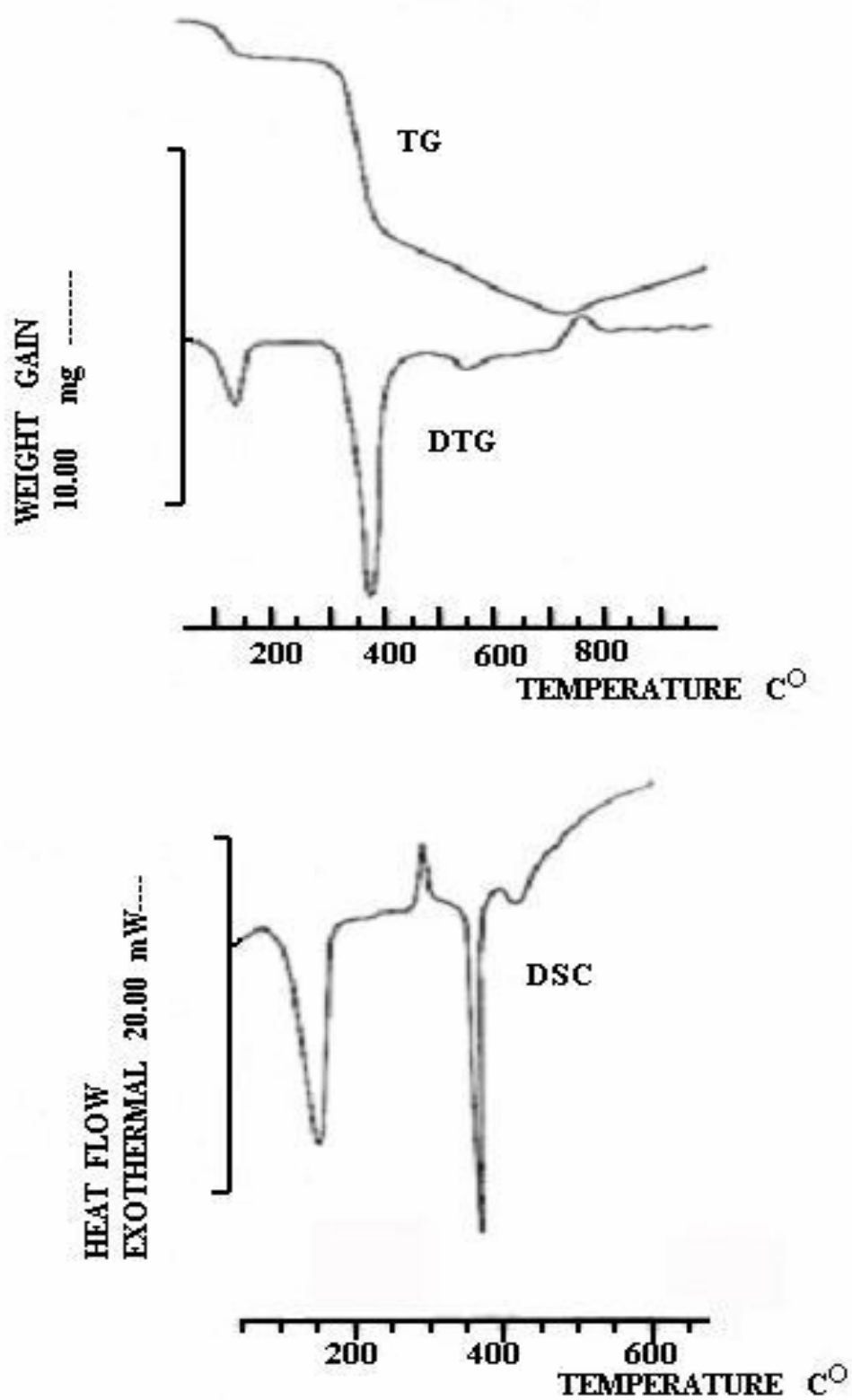


Fig.3. TG, DTG and DSC curves for cobalt cinnamate .

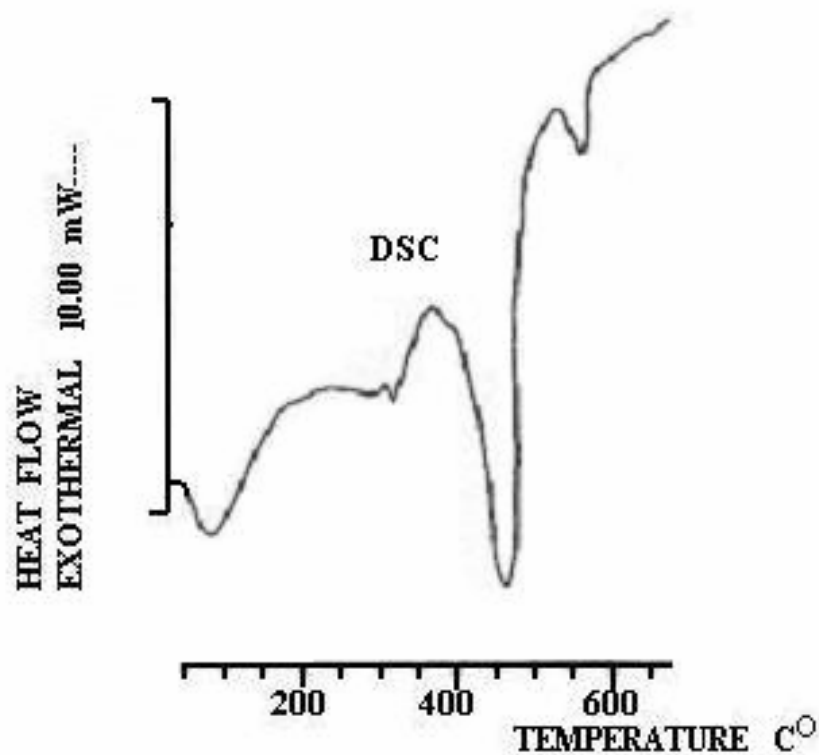
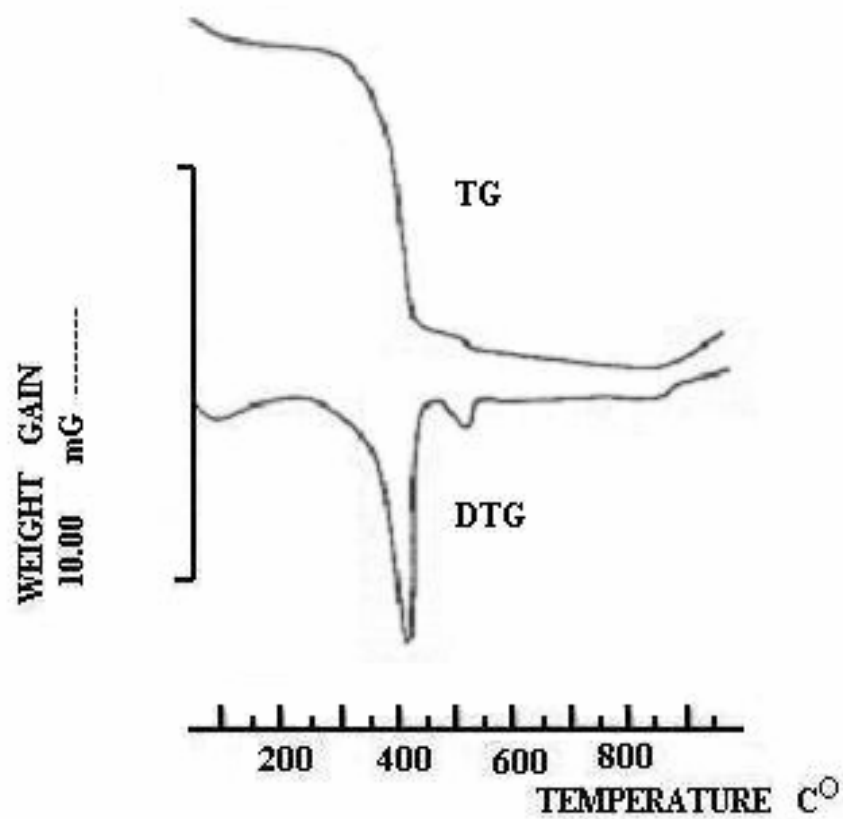


Fig.4. TG, DTG and DSC curves for nickel cinnamate .

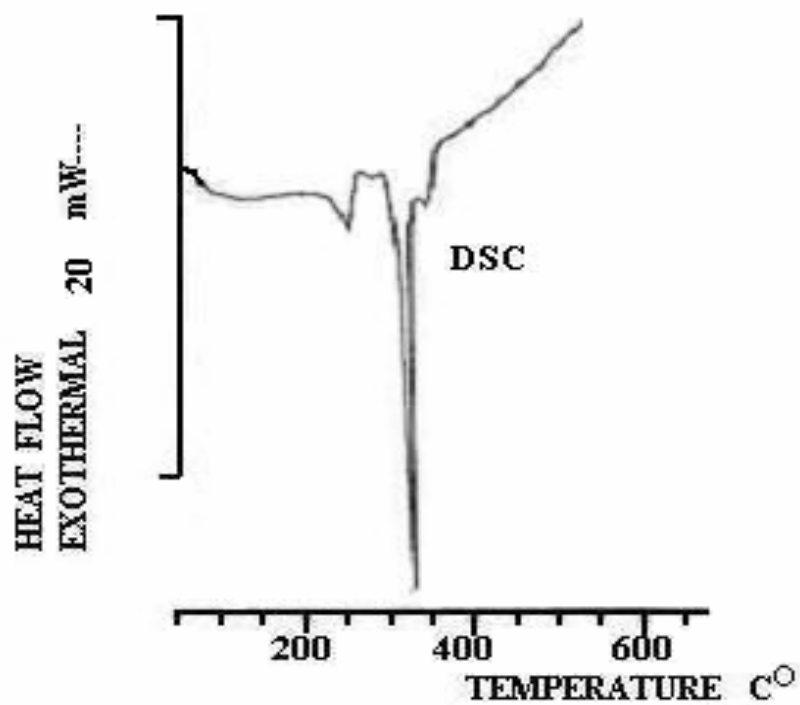
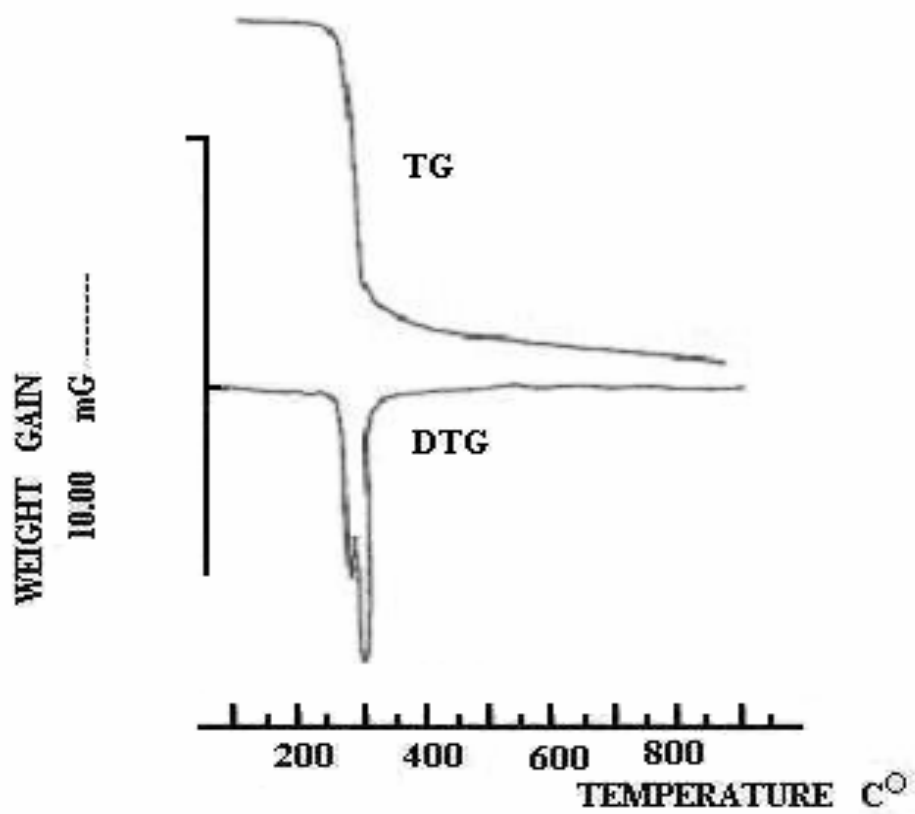


Fig. 5. TG, DTG and DSC curves for copper cinnamate .

REFERENCES

1. S.P.Goel, S.Kumar and M.P. Sharma, *Thermochem. Acta*, 188 (1991) 201.
2. H. Langbein and S. Fischer, *Thermochem. Acta*, 182 (1991) 39.
3. A.K. Galwey, M. Mohamed, S. Rajim and M.E. Brown, *J. Chem. Soc. Faraday Trans. I*, 84 (1988) 1349.
4. N.J.Carr and A.K. Galwey, *J. Chem. Soc. Faraday Trans.I*, 84 (1988) 1357.
5. J.R. Allan, B.R. Carson, D.L. Gerrard and S. Heoy, *Thermochem. Acta*, 154 (1989) 315
6. A.R. Salvador, E.G. Galvo and P. Leton, *Thermochem. Acta*, 154 (1989) 263.
7. R.C. Stoufer, D.W. Smith, E.A. Clevenger and T.E. Norris, *Inorg. Chem.*, 5 (1966) 167.
8. L.S. Forster and C.J. Ballhausen, *Acta Chem. Scand.*, 16 (1962) 1385.
9. J.R. Allan, N.D. Baird and A.L. Kassyk, *J. Therm. Anal.*, 16(1979) 79.
10. J. Sestak and G. Berggren, *Thermochem. Acta*, 3 (1971) 1.
11. V. Satava, *Thermochem. Acta*, 2 (1971) 423.
12. A.W. Coats and J.P. Redfren, *Nature*, 201 (1964) 68.
13. J.W Moore and R.G. Pearson, *Kinetics and Mechanism*, 3rd edn. Wiley, New York, 1981, P.181.

